

Parametric Analysis and Optimization of Sinker-EDM Process for High Tensile Strength Steel Using Response Surface Methodology

Sukarman¹, Muhamad Taufik Ulhakim¹, Khoirudin¹, Dodi Mulyadi¹, Amir¹, Danang Supriyanto¹, Rohman^{2*}, Amri Abdulah².

¹Department of Mechanical Engineering, Faculty of Engineering, Universitas Buana Perjuangan Karawang, Jl. HS.Ronggo Waluyo, Puseurjaya, Telukjambe Timur, Karawang, West Java, 41361, Indonesia.

²Department of Mechanical Engineering, STT Wastukencana, alan Cikopak No.53, Mulyamekar, Purwakarta, West Java, 41151, Indonesia.

ABSTRACT

This investigation focuses on optimizing the sinker electrical discharge machining (sinker-EDM) process parameters for high tensile strength steel (HTSS), specifically SKD-11, utilizing Box-Behnken Response Surface Methodology (BB-RSM). In the manufacturing of molds, dies, and components for sectors like automotive and aerospace, Sinker-EDM is a commonly used technique. This process eliminates direct contact between the electrode and the workpiece. However, its low material removal rate (*MRR*) constrains productivity was set as respond variable. This research endeavors to enhance *MRR* by employing rectangular graphite electrodes. The BB-RSM was utilized to evaluate the effects of input parameter including of pulse current, spark-on time, and gap voltage on *MRR*. The optimal *MRR* of 45.49 mm³/min was attained at a pulse current of 16 A, spark-on time of 400 μ s, and gap voltage of 45 V. ANOVA revealed that *MRR* more significantly influences pulse current and spark-on time than gap voltage. Interaction and surface plot analyses confirmed that high pulse current and extended spark-on time resulted in the maximum *MRR*. These findings provide valuable insights for optimizing the sinker-EDM process for SHTSS, contributing to enhanced productivity and efficiency in manufacturing.

Keywords: Box-Behnken Response Surface Methodology, High tensile strength steel, Mmaterial removal rate, Sinker-EDM.

Article information:

Submitted: 29/01/2025

Revised: 01/02/2025

Accepted: 08/02/2025

Published: 15/02/2025

Author correspondence:

* ✉:

Rohman@wastukencana.ac.id.

Type of article:

☒ Research papers

☐ Review papers

This is an open access article under the [CC BY-NC](https://creativecommons.org/licenses/by-nc/4.0/) license



1. Introduction

Sinker electrical discharge machining (sinker-EDM) is a non-traditional process that removes material from a workpiece using an electrode tool to create precise dimensions and shapes [1]. Sinker-EDM is extensively used to produce dies, molds, and spare parts in the automotive and aerospace industries [2, 3]. Machining errors associated with tool electrode deformation, vibration-related inaccuracies, chatter, and mechanical stresses are mitigated because of the absence of direct contact between the workpiece and tool electrode during the sinker-EDM process [4]. The tools and materials employed for material removal are immersed in a dielectric medium [5]. This study was conducted by machining a newly developed hardened carbon steel. The sinker-EDM machine regulates the movement of the electrode tool to erode the material by generating high-frequency electric sparks [6]. Sinker-EDM can eliminate the chatter, mechanical stress, and vibration issues prevalent in traditional machining methods [7]. The most significant challenge during the sinker-EDM process is the flushing or removal of eroded particles in the interelectrode gap. The residual material deposited in the cavity of the workpiece and electrode can lead to distortion and short circuiting.

The surface finish (surface profile) and integrity of the resulting workpiece significantly influence the material removal rate (*MRR*) during the sinker-EDM process [8].

Pulse current, pulse-on time, pulse-off time, and gap voltage are adjustable parameters in the sinker-EDM process. The peak current and pulse-on time are critical parameters in sinker-EDM [8]. The pulse-on time refers to the interval of electrical discharge between the electrode and the work material once the dielectric breakdown voltage is reached, ionizing the dielectric [9]. This discharge causes material deterioration on the workpiece surface [10]. The pulse-off time represents the period without an applied electrode voltage. Reducing the pulse-off time increases the pulse-on time, thereby enhancing the discharge efficiency, sparking consistency, and cutting rate [11]. However, very short pulse-off times can lead to wire rupture and unstable discharges. When the sparking became unstable, increasing the pulse-off time reduced the pulse duty factor and average gap current. The peak current is the maximum current provided by the power supply for each pulse [12]. The average current in the spark gap was measured throughout a single cycle and recorded using a machine meter during machining. A spark in sinker-EDM is generated when the discharge erodes the workpiece [4]. The gap voltage refers to the alternating voltage between the electrodes and determines the total energy of the applied spark [13]. Sinker-EDM was time intensive because each discharge removed only a small amount of material. In response to this challenge, scholars have formulated mathematical models to estimate the material removal rate (*MRR*) by considering both material characteristics and process parameters. Investigations revealed that the *MRR* in sinker-EDM exhibited a direct correlation with the peak current. Notably, the shape of the current-time profile demonstrated a minimal impact on the *MRR*, suggesting a lack of sensitivity to variations in on-time and off-time conditions.

Several studies have investigated methods for enhancing the quality and productivity of sinker-EDM processes [14–18]. Swiercz *et al.* [14] utilized the Taguchi method combined with response surface methodology (RSM) to optimize machining parameters such as pulse-on time, discharge current, and pulse current for heat-treated tool steel (55 HRC) using copper electrodes. Their findings demonstrated that the *MRR* and surface roughness (*Ra*) were critical response variables, achieving *Ra* values between 1.0 and 2.0 μm with optimal roughness determined through a desirability approach. Al Akbari and Baseri [15] evaluated the effects of pulse current, pulse-on time, and electrode rotation on *MRR*, *Ra*, overcut, and electrode wear rate (EWR) using a Taguchi design with three levels. The analysis was conducted on the X210Cr12 (SPK) work material and pure copper electrodes, and the pulse current and pulse-on time were identified as the most significant parameters influencing the machining performance. Sultan *et al.* [16] applied RSM to optimize *MRR*, *Ra*, and EWR using EN 353 steel and pure copper electrodes, achieving optimal values for EWR (6.47 mm^3/min), *MRR* (17.62 mm^3/min), and *Ra* (4.54 μm) at specific parameter settings, including a pulse-on time of 100.77 μs and peak current of 45 A. Similarly, Chandramouli *et al.* [17] studied the effects of peak current, pulse-on time, and pulse-off time on *MRR* and *Ra* for precipitation-hardened stainless steel using tungsten-copper alloy electrodes, with the Taguchi design and ANOVA confirming the significant influence of these parameters on machining outcomes. Sumanto *et al.* [18] further investigated the impact of input parameters on the surface roughness and overcut diameter using an SPHC (JIS 3131) work material and graphite electrodes, demonstrating the potential of the Taguchi method for evaluating machining performance and enhancing productivity. The approach in SEDM utilizing BB-RSM offers the advantage of analyzing factor interactions, thereby enabling the modeling of more complex relationships between the process variables and responses. BB-RSM differs from the Taguchi method, which primarily focuses on determining the optimal combination of parameters with a minimal number of experiments without extensively considering the effects of interactions between factors [19]. BB-RSM provides a more comprehensive understanding of the influence of parameters such as current, pulse time, and voltage on the surface roughness or electrode wear rate in SEDM.

Despite extensive research on sinker-EDM, there remains a significant gap in the literature regarding the optimization of the Material Removal Rate (*MRR*) for hardened SHTSS (JIS G4404) materials in this process. This study employed the Box-Behnken response surface methodology (BB-RSM) to optimize the

process parameters for the specified material. RSM is recognized for its capacity to minimize process variation through robust experimental design, rendering it an effective tool for manufacturing process optimization. This non-traditional approach presents a cost-effective alternative to conventional production methods, making it suitable for enhancing sinker-EDM productivity. The investigation focused on three input parameters: pulse current (I), spark-on-time (T_{on}), and gap voltage (V_g), with experimental maximum-minimum levels applied as required using the BB-RSM method. In this study, SHTSS (JIS G4404) was used as the workpiece material, and a rectangular graphite electrode was used for machining. The primary objective was to identify the optimal sinker-EDM parameters to maximize the *MRR*, which is expected to enhance the overall process productivity. By adhering to the recommended sinker-EDM process parameters, this study successfully determined the optimal settings for enhancing *MRR* using a rectangular graphene electrode. These findings provide critical insights for optimizing sinker-EDM operations and improving process efficiency.

2. Methods

2.1. Experimental preparation and setup

The sinker-EDM (S-EDM) process is evaluated based on key performance indicators, including the *MRR*, workpiece surface finish, and overcut dimensions [20, 21]. The primary machining parameters that influence these metrics are discharge current, pulse duration, pulse frequency, wire speed, wire tension, and dielectric flow rate.

In this study, SHTSS was selected as the workpiece material. The chemical composition and mechanical properties conform to the JIS G 4404 standard [22]. The material was subjected to preparation processes, including stamping, hardening, and subsequent machining using sinker-EDM. A rectangular graphite electrode was selected because of its superior electrical conductivity and high thermal stability. The electrodes were prepared with precise dimensions before the machining experiments were conducted.

The machining process was performed using a C-TEK ZNC-50A sinker-EDM machine, which is known to exhibit high precision and stability. The measurement instruments included a digital weighing scale used to record the mass of both the workpiece and electrode before and after machining, as well as a stopwatch for accurately tracking the machining time. Figure 1 illustrates the outcomes of the sinker-EDM process conducted using a C-TEK ZNC-50A machine.

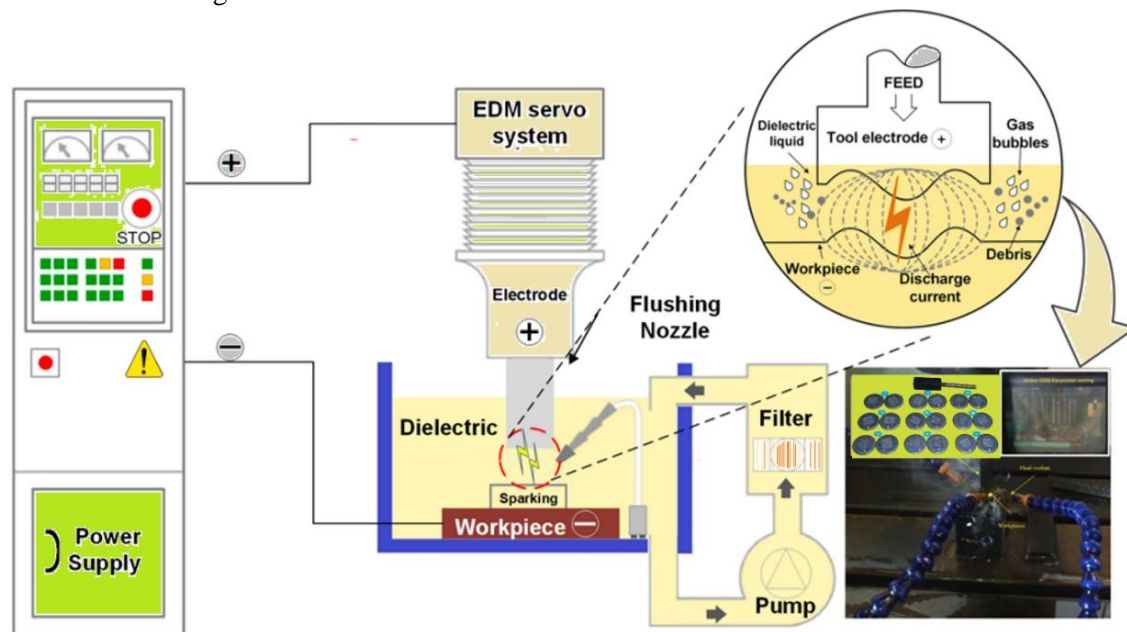


Figure 1. Schematic of sinker-EDM in C-TEK ZNC-50A machine.

During the machining process, a sinker-EDM apparatus was equipped with a rectangular graphite

electrode that generated high-voltage electric sparks to erode the workpiece material. The dielectric fluid was continuously circulated through the gap between the electrodes to remove debris and maintain stable thermal conditions. Repeated sparking and controlled material erosion enabled the precise shaping of the workpiece. The uniformity of the rectangular graphite electrode is crucial for maintaining consistent machining results. Fluctuations in the electrode material characteristics can result in uneven machining performance, affecting the dimensional precision and surface quality. In contrast, the rectangular graphite electrode exhibited superior material uniformity, which facilitated steady operation and produced a high-quality surface finish. This uniformity is essential for obtaining reliable machining results.

The sinker-EDM process involves controlling the input parameters for each iteration, as outlined in Table 1. The sinker-EDM processing time (t) for each iteration is set to 5 min. The erosion of the work material during each run was measured in grams per minute by calculating the difference in the weight of the material before and after the process and dividing this difference by the processing time. This method followed the approach confirmed in previous studies [10, 18].

Table 1. RSM Matrix for optimizing the material removal rate in sinker-EDM

Code	Sinker-EDM Parameters	Symbol	Level	
			Min	max
A	Pulse current, A	I	10	16
B	spark on time, (μ s)	T_{on}	210	400
C	Gap voltage, V	V_g	40	50

A = Ampere, μ s = micro second, and V= Volt

2.2. Experimental design

The widespread application of BB-RSM in optimizing production processes and conducting scientific research can be attributed to its robust experimental design. This approach effectively minimizes variations across diverse fields, including resistance spot welding [23, 24], paint optimization [25], and machining [26]. BB-RSM allows data collection using the smallest possible sample size by identifying key input parameters that significantly impact product quality or research outcomes. The main goal of BB-RSM is to reduce process variation while enhancing output quality and lowering costs [27]. Through its systematic experimental design, RSM helps to determine the influence of various parameters on the mean and standard deviation of process performance metrics, which serve as indicators of process efficiency.

In BB-RSM, the experimental design utilizes orthogonal arrays to systematically arrange the influential parameters and their corresponding levels, thereby ensuring that effective variation is generated using statistical software. Instead of conducting comprehensive tests on all possible parameter-level combinations, BB-RSM employs a strategic approach by selecting a critical yet limited subset of combinations. This methodology yields valuable data for identifying the most significant parameters affecting product quality while concurrently reducing the number of requisite experiments. Consequently, BB-RSM effectively minimizes time and resource utilization without compromising the accuracy of the results.

2.2.1. The parameter otimization

Optimization of the matrix parameters (OMP) enabled a balanced comparison among the parameters and allowed for the accurate selection of samples from specific groups, although it represented only a fraction of the full factorial experiment. OMP facilitates experimental planning and data analysis by maximizing the information obtained regarding influential parameters while minimizing the number of experiments. One of the primary advantages of OMP is its ability to identify significant parameters with minimal testing, thereby reducing both time and cost during trials [28-30].

The number of experiments in the BB-RSM design was represented by Lm where m denoted the total number of parameters, and L indicated the number of levels for each factor. Several experiments involved

multiple parameters with varying levels, necessitating an efficient factorial design. This requirement was addressed by using an orthogonal array that minimized the number of factor-level combinations. **Table 1** illustrates the OMP L9 (3^3) implementation for RSM, incorporating three parameters and three experimental levels, yielding eight degrees of freedom. To ensure the reliability of the results, all RSM design iterations were conducted twice to improve data accuracy.

2.2.2. Material removal rate

In the sinker-EDM process, *MRR* is a vital parameter for evaluating productivity and quantifying the volume of material removed per unit time. As machining productivity is directly proportional to the *MRR*, achieving a high *MRR* significantly enhances the overall process efficiency.

In this study, the sinker-EDM process was performed in five-minute test iterations. The mass of the workpiece was measured before (W_0) and after machining (W_1) using an electronic weighing scale with a precision of 0.001 g, and a stopwatch was used to verify the machining duration. The *MRR* was calculated using Equation 1 [18, 31].

$$MRR = \frac{W_0 - W_1}{t \cdot \rho} \quad (1)$$

where *MRR* is the material removal rate ($\text{mm}^3/\text{minutes}$), t is the machining time (min), and ρ is the density of the working material density (grams/cm^3), respectively.

The sinker-EDM process enables precise material removal through controlled spark erosion, with *MRR* influenced by key input variables such as pulse current, spark-on time, and gap voltage. The selection of an optimal combination of these variables is essential for each experiment to achieve reliable and efficient machining outcomes.

2.2.3. Signal- to-noise ratio (S//N ratio)

Experiments were conducted using a Design of Experiments (DOE) approach developed using BB-RSM. This methodology provides a robust experimental framework with minimal trials to achieve optimal results, making it a widely employed approach for various manufacturing systems. Its application facilitates an efficient analysis of the effects of machining variables on selected responses while minimizing costs and time [5]. The first step employs the S/N ratio to identify the direction of parameter adjustments, whereas the second step determines the control input required to achieve the desired mean response with an optimal effect on the S/N ratio. The S/N ratio for "Larger is better," "Smaller is better," and "Nominal is the best" can be calculated by Equation (2), (3), and (4), respectively [28, 30, 32].

Larger is better:

$$S/N \text{ ratios} = -10 \log \frac{1}{n_0} \sum_{i=1}^{n_0} \frac{1}{y_i^2} \quad (2)$$

Smaller is better:

$$S/N \text{ ratios} = -10 \log \sum_{i=1}^{n_0} \frac{y_i^2}{n_0} \quad (3)$$

Nominal is the best:

$$S/N \text{ ratios} = -10 \log \frac{\bar{y}^2}{s^2} \quad (4)$$

The S/N ratio measures the fluctuations in the response relative to the target value under various noise conditions. As outlined in this study, the quality characteristic follows the "larger is better" principle, implying that higher S/N ratios correspond to superior performance [36].

2.2.4. Analysys of Variant (ANOVA)

Analysis of variance (ANOVA) is a statistical technique used to partition the observed variance in a dataset into components attributable to different sources, enabling further statistical testing [33]. This method is particularly effective for analyzing the relationships between the dependent and independent variables. In this study, a two-way ANOVA was employed to evaluate the influence of the machining parameters on the *MRR*. The analysis was conducted using datasets comprising three or more groups, with a 95% confidence level. A p-value threshold of 0.05 was set to identify statistically significant parameters [34-36].

2.2.5. Interaction plot parameters

Examining the interaction plot parameters aims to identify the machining process elements and their interplay, which significantly affects the process outcomes [17]. An Interaction Plot illustrates how a second categorical variable modifies the relationship between a variable and continuous response. The x-axis displays the means for the levels of one factor, whereas the different lines represent the means for the other parameters [27]. An analysis of these lines reveals the impact of interactions on the variable-response relationship. Parallel lines indicate no interaction, whereas nonparallel lines indicate the presence of an interaction. The strength of the interaction correlates with the degree of nonparallelism.

3. Results and Discussion

3.1. Material removal rate analysis

The *MRR* study examined key sinker-EDM parameters, including discharge current (I_p), spark-on time (T_{on}), and gap voltage. The reduced pulse current diminished the discharge energy, creating shallower cavities and enhancing debris removal. Conversely, an increased peak current amplifies the discharge energy, producing deeper cavities. However, debris accumulation in these deeper cavities leads to short-circuiting and disrupted electrical discharge, thereby lowering the *MRR* [35]. Optimizing the *MRR* requires identifying an ideal pulse current that balances the discharge energy and debris expulsion. Figure 2 illustrates the 18 test samples for each sinker-EDM process. The study evaluated a total of 18 samples labeled as R1.1, R2.1, R1.2, R2.2, R1.3, R2.3, R1.4, R2.4, R1.5, R2.5, R1.6, R2.6, R1.7, R2.7, R1.8, R2.8, R1.9, and R2.9.

The experimental *MRR* data were obtained by calculating the mass of the removed work material for each sample. The results showed a clear trend: the *MRR* was at a minimum during the first iteration, gradually increased, and reached a maximum during the ninth iteration. This pattern highlights the influence of machining parameters on material removal rates and the importance of parameter optimization for maximizing productivity.

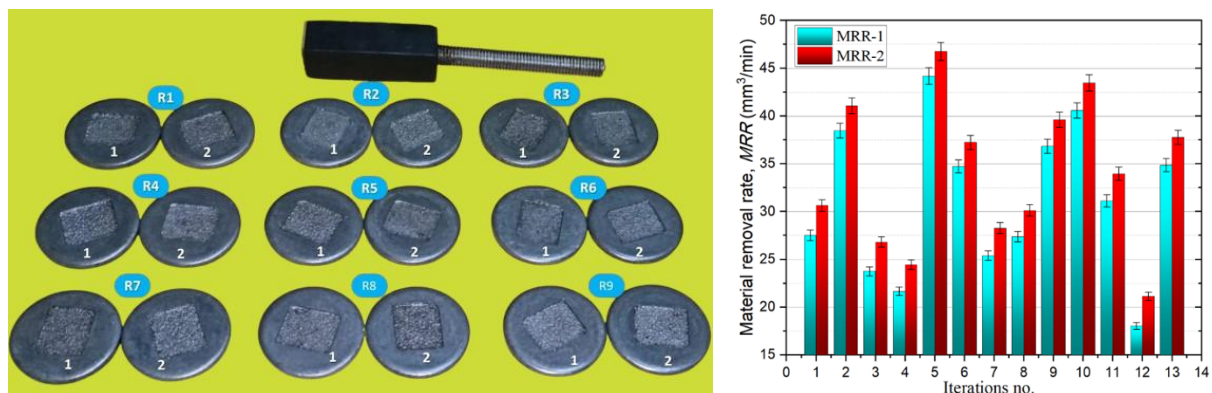


Figure 2. Material removal rate: (a) sinker-EDM sample of high tensile strength steel (SHTSS) work material with graphene electrode; (b) material removal rate (*MRR*) results.

These findings align with those of previous studies and the fundamental theory of sinker-EDM applications [6]. A relationship between the pulse current and *MRR* was observed. As the pulse-current magnitude increased, the *MRR* exhibited a corresponding increase. This phenomenon can be attributed to elevated spark energy, which facilitates enhanced melting and vaporization at the machining interface. The increased spark energy promoted a higher discharge frequency, contributing to the accelerated material removal. However, excessive pulse currents can lead to debris accumulation in the spark gap, affecting discharge stability and causing a decline in productivity. Therefore, optimizing the pulse current is essential to achieve the maximum *MRR* without compromising machining performance.

The experimental results for the *MRR* obtained in this study are summarized in Table 2, which provides an overview of the material removal rate variations across different parameter settings. This table highlights

the significant impact of the machining parameters, particularly the pulse current, on the *MRR*. These observations reaffirm the sinker-EDM machining principles and provide insights into improving the process efficiency.

3.2. S/N ratio analysis

The *MRR* is a critical response in the sinker-EDM process for evaluating productivity and efficiency, as shown in Table 2. The analysis revealed that the highest *MRR* occurred in Run 5, with a pulse current of 16 A, spark-on time of 400 μ s, and gap voltage of 45 V. This combination resulted in an average *MRR* of 45.49 mm³/min, corresponding to the highest S/N ratio of 33.1464. These findings indicate that a high pulse current, extended spark-on time, and medium-gap voltage yield optimal material removal. Conversely, the lowest *MRR* was observed in Run 12, with an average of 19.60 mm³/min and the lowest S/N ratio of 25.76, resulting from low pulse current (10 A), short spark on time (210 μ s), and medium gap voltage (45 V).

Table 2. Material removal rate of sinker-EDM

Run No.	Pulse current, A	Input parameters		<i>MRR</i> (mm ³ /minutes)		S/N Ratio
		Spark on time, (μ s), B	Gap voltage, V, C	R ₁	R ₂	
1	13	210	50	27.51	30.65	29.2342
2	16	305	40	38.47	41.09	31.9792
3	10	305	50	23.77	26.82	28.0133
4	10	305	40	21.66	24.44	27.2054
5	16	400	45	44.20	46.77	33.1464
6	13	400	40	34.73	37.26	31.1085
7	13	210	40	25.40	28.27	28.5366
8	10	400	45	27.38	30.12	29.1434
9	13	400	50	36.85	39.63	31.6329
10	16	305	50	40.59	43.46	32.4550
11	13	305	45	31.12	33.95	30.2229
12	10	210	45	18.05	21.14	25.7606
13	16	210	45	34.86	37.78	31.1827

These results suggest that the pulse current exerts the most significant influence on the *MRR*, as increased current enhances the discharge energy, accelerating material removal. An extended spark-on time yields a higher *MRR* owing to the prolonged energy-discharge duration. However, the effect of the gap voltage on the *MRR* is complex, with a medium value (45 V) demonstrating superior performance compared to low (40 V) or high (50 V) values. This optimal gap voltage likely facilitates improved spark discharge stability, enhancing the material removal efficiency. The parameter combination producing the highest *MRR* and optimal stability was observed at a pulse current of 16 A, spark-on time of 400 μ s, and gap voltage of 45 V, as shown in run 5. This combination may be recommended as the optimal parameter configuration in the sinker-EDM process to achieve maximum material removal efficiency.

To achieve an optimal MMR, it is advisable to utilize all parameters under the maximum conditions, as indicated in Figure 3. This finding aligns with the observations of Sultan *et al.* [15], who demonstrated the same trend using RSM. At lower pulse currents, the generated heat is minimal, mostly absorbed by the surrounding environment and machine components, with only a small fraction used to melt and evaporate the working material. Higher pulse currents resulted in a more significant energy discharge, enhancing the material removal process. S/N ratio analysis confirmed that as the *MRR* increased, the experimental quality improved, as reported in previous studies [15, 16].

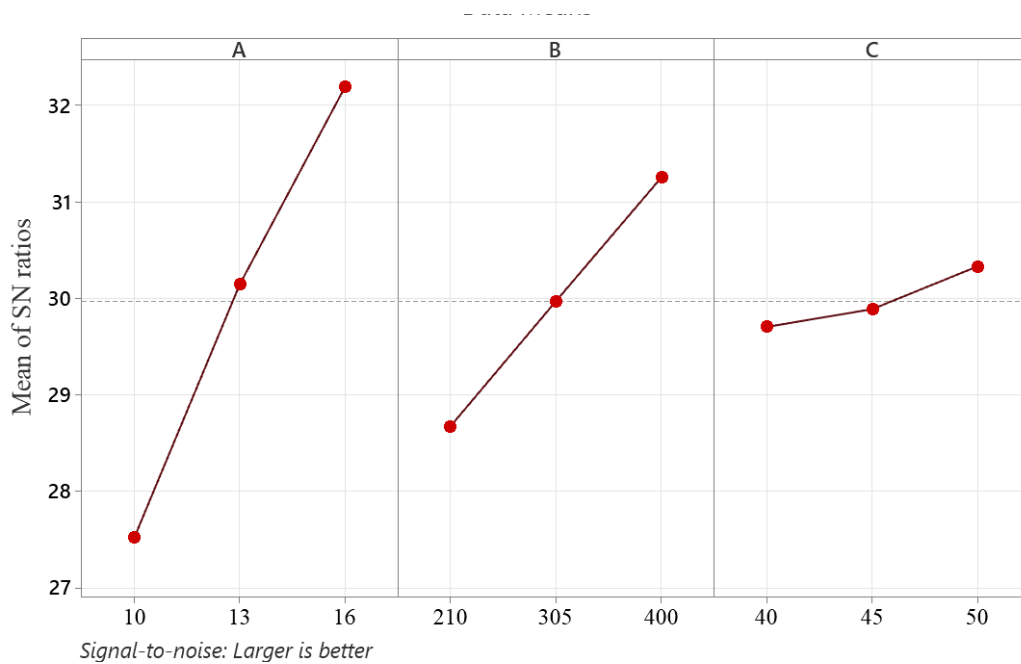


Figure 3. The S/N ratio of sinker-EDM parameters

3.3. Analysis of variance (ANOVA)

Table 3 shows the results of the ANOVA for the *MRR*, demonstrating that the pulse current and spark on the time parameters exert a significant effect on the *MRR*, while the gap voltage exhibits an insignificant effect at the 95% confidence level. The table indicates that the pulse current has an F value of 233.01, with a p-value <0.001, suggesting that this factor is the most influential variable affecting the *MRR* [5, 37-39]. This observation aligns with the principles of the EDM technique, where a higher current leads to a greater energy discharge, thereby enhancing the material removal rate. Moreover, the spark-on time demonstrated an F value of 71.13, with a P value <0.001, which also indicated a significant effect on the *MRR*. An extended spark-on time facilitates a prolonged energy release, thereby enhancing the material removal process. Conversely, the gap voltage exhibits an F value of 4.19, with a P value of 0.073, indicating that its effect on the *MRR* is not statistically significant at the 95% confidence level. This observation suggests that the gap voltage exerts only a minimal influence on spark stability and productivity.

Table 3. The ANOVA for *MRR* of sinker-EDM

Parameter Code	DF	Seq SS	Adj MS	F	P
Pulse current,	2	43.6859	43.6602	233.01	0
Spark on time, (μs)	2	13.3345	13.3281	71.13	0
Gap voltage, V	2	0.7849	0.7849	4.19	0.073
Residual Error	6	0.5621	0.5621	233.01	0
Total	12	58.3674			

A total Seq SS value of 58.3674 indicates total variation in the *MRR* data that can be explained by the model. Pulse current contributed the most to the variation, with a Seq SS value of 43.6859, accounting for 74.8% of the total contributions, followed by spark-on time with a Seq SS value of 13.3345 (22.9%), whereas gap voltage contributed only 0.7849 (1.3%). Furthermore, the residual error had a Seq SS value of 0.5621, indicating that the variation in data not explained by the model was minimal, suggesting that this model can be considered valid and representative for evaluating *MRR* parameters. This study corroborates previous findings, emphasizing the critical influence of pulse current on the *MRR* [10, 16, 18, 40].

3.4. Interaction plot analysis of process parameters on *MRR*

The interaction plot illustrates the relationship between the three sinker-EDM process parameters, pulse current (A), spark-on time (B), and gap voltage (C), and their effects on the *MRR*. The nonparallel line patterns in Figure 4 indicate the interactions between these parameters.

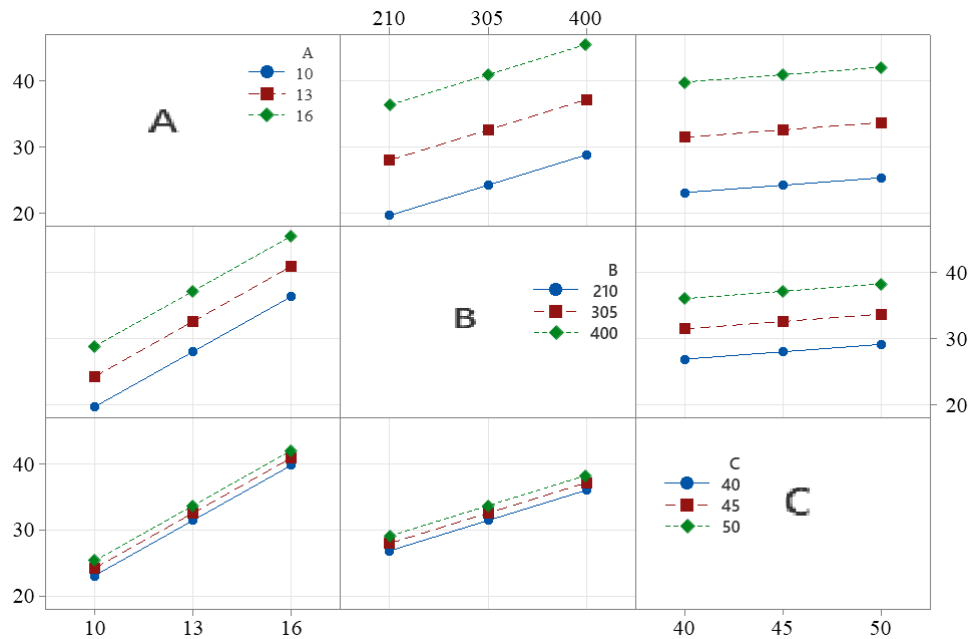


Figure 4. Interaction plot parameter of sinker-EDM

3.4.1. Interaction of pulse current and spark-on time ($A \times B$)

The graph in subplot A-B shows that increasing the spark-on time (from 210 to 400 μ s) increased the effect of the pulse current on the *MRR*. At a current of 16 A, the *MRR* increased significantly compared to that at a current of 10 A, especially at higher spark-on times. This demonstrates a positive interaction between the two parameters, indicating that a larger pulsed current is more effective when the spark-on time is extended.

3.4.2. Interaction of pulse current and gap voltage ($A \times C$)

In subplots A-C, the effect of the pulse current on the *MRR* was relatively consistent across all gap voltage levels. However, increasing the pulse current resulted in a significant increase in the *MRR*. The misalignment of the lines at a certain gap voltage level (e.g., 50 V) is smaller than that of the A-B interaction, indicating a moderate interaction between these two parameters.

3.4.3. Interaction between spark-on time and gap voltage ($B \times C$)

The B-C subplot shows that the spark-on time had a significant effect on the *MRR*, whereas the effect of the gap voltage was smaller. The lines are almost parallel, indicating that the interaction between these two parameters is weak. The main effect of the spark-on time on the *MRR* was more dominant than that of the gap voltage.

Overall, the interaction plot results show that the combination of a high pulse current and a long spark-on time provides the largest contribution to the *MRR*. The gap voltage had a smaller effect and tended not to show a significant interaction with the other parameters.

3.5. Surface and countour plote analysis

Figure 5 illustrates the interaction between three critical parameters in the material removal process: pulse current, spark-on time, and gap voltage, and their effects on the *MRR*, which can be further analyzed. In Figure 5 (a), examining the interaction between the pulse current (A) and spark-on time (B), increasing the pulse current consistently enhanced the *MRR*, with a more pronounced effect when the spark-on time

increased from 200 μs to 400 μs . The positive interaction indicates that combining a high pulse current and extended spark-on time yields the maximum *MRR*, suggesting that these factors synergistically contribute to a higher sinker-EDM efficiency.

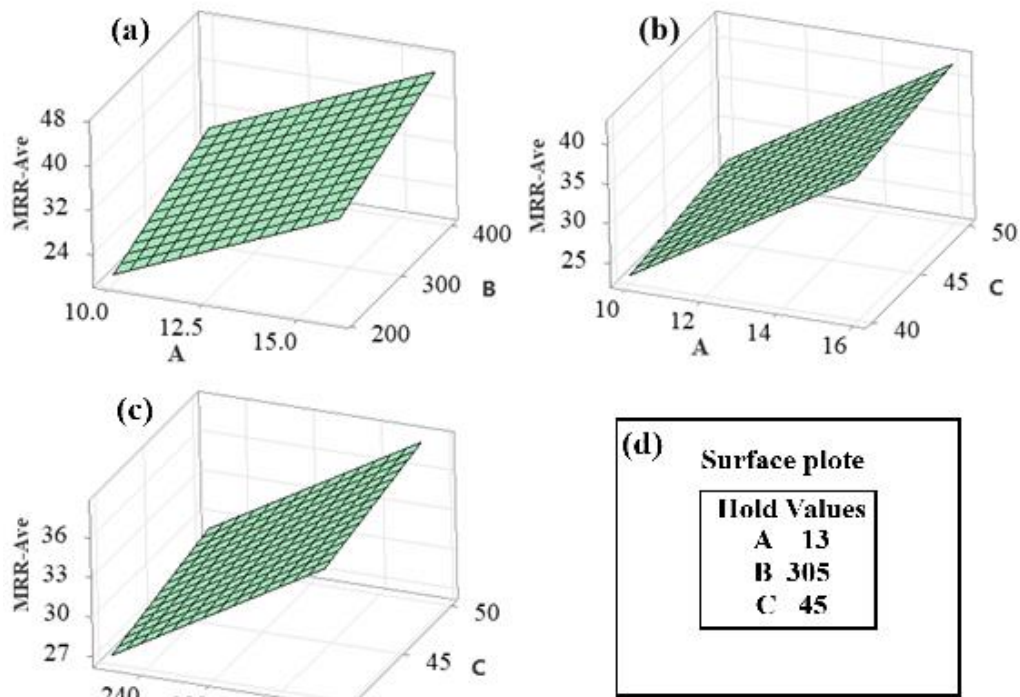


Figure 5. Surface plot parameter of sinker-EDM.

The subplot in Figure 5 (b), depicting the interaction between the pulse current (A) and gap voltage (C), demonstrates that increasing the pulse current enhances the *MRR*, although the effect of the gap voltage is less substantial. The gap voltage exhibits a minor effect, as variations do not induce significant changes in the *MRR* compared to the effect of the pulse current. The subplot in Figure 5 (c), which illustrates the interaction between the spark-on time (B) and the gap voltage (C), demonstrates that the *MRR* increases with increasing spark-on time. The gap voltage marginally affected the *MRR*; however, its effect was less pronounced than that of spark-on time. An extended spark-on time with a medium-to-high gap voltage tends to produce optimal *MRR* values, although the role of the gap voltage is limited. Figure 5 (d) shows the fixed values for each parameter in each subplot: the gap voltage was 45 V, spark-on time was 305 μs , and pulse current was 13 A.

The contour plot in Figure 6 shows the interplay between three key parameters in material removal: pulse current, spark-on time, and gap voltage, and their impact on the Material Removal Rate (*MRR*). This interaction can be further examined using surface plots of the sinker-EDM parameters. Figure 6 (a) reveals that as the pulse current (A) increased, the *MRR* consistently improved, with a more noticeable effect when the spark-on time (B) increased from 200 μs to 400 μs .

The positive interaction suggests that combining a high pulse current and extended spark-on time maximizes the *MRR*, indicating a synergistic effect on the material removal efficiency. In Figure 6 (b), the interaction between the pulse current (A) and gap voltage (C) shows that while increasing the pulse current enhances the *MRR*, the gap voltage has a less significant impact. Gap voltage variations induce minimal changes in the *MRR* compared with the pulse current effects. Figure 6 (c) demonstrates that the *MRR* increases with a longer spark-on time (B), while the gap voltage (C) has a marginal effect, which is less pronounced than the spark-on time. Optimal *MRR* values tend to result from extended spark-on time and medium-to-high gap voltage, though gap voltage plays a limited role. Figure 6 (d) displays the fixed values for each parameter in the subplots: 45 V for gap voltage, 305 μs for spark-on time, and 13 A for pulse current.

The analysis revealed that the pulse current (A) exerted the strongest influence on the *MRR*, followed by the spark-on time (B), while the gap voltage (C) had a minor effect. High levels of pulse current and spark-on time yielded the greatest material removal efficiency, whereas gap voltage variations minimally affected the *MRR*.

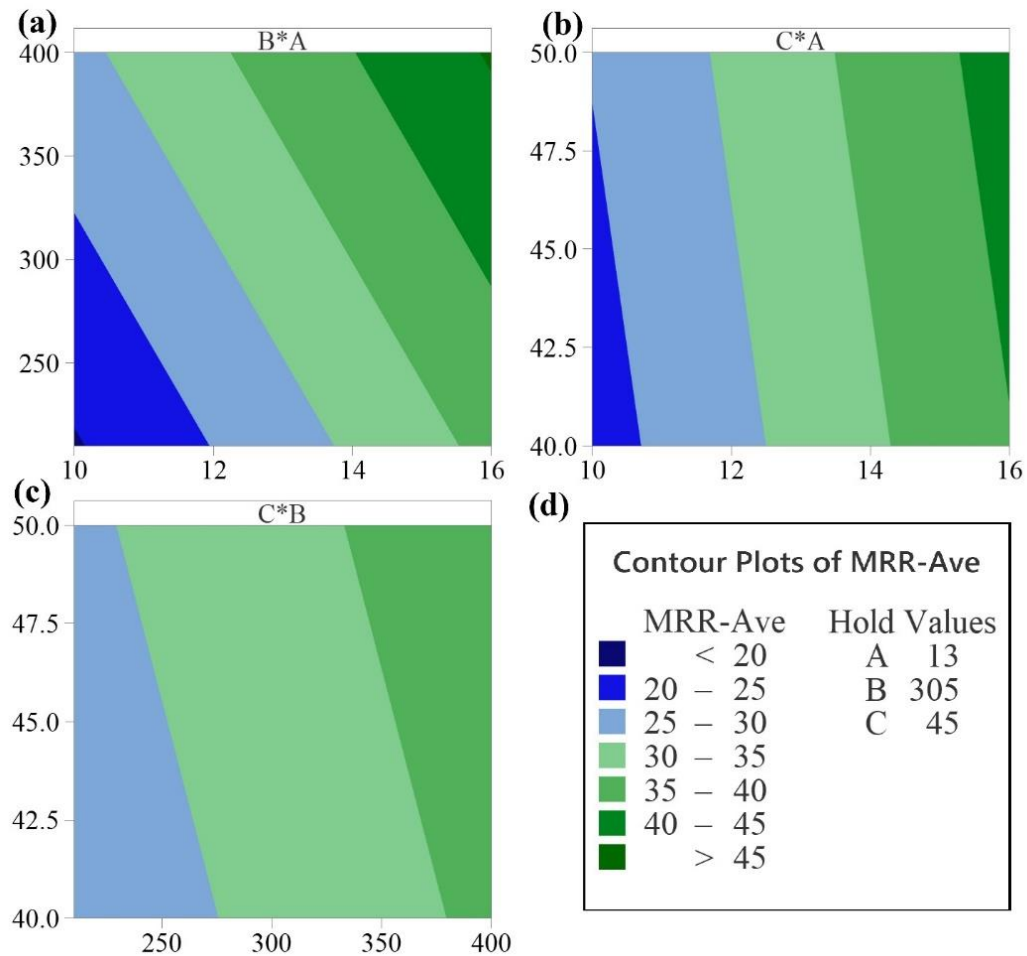


Figure 6. Countour plot parameter of sinker-EDM

4. Conclusions

Sinker-EDM is widely used for manufacturing precision components, although it generally exhibits a lower material removal rate (MRR) than conventional machining. The MRR in sinker-EDM is influenced by the material properties, electrode geometry, and discharge parameters. This study optimized the process for high-tensile-strength steel (SHTSS) using the Box-Behnken Response Surface methodology (BB-RSM) using the following results:

- The highest MRR of 45.49 mm³/min was achieved with a pulse current of 16 A, spark-on time of 400 μs, and gap voltage of 45 V.
- The ANOVA results confirmed that the pulse current and spark-on time had significant effects on the MRR, while the gap voltage had a minimal impact.
- Interaction and surface plot analyses further confirmed that a higher pulse current and extended spark-on time maximize the MRR.
- The optimal parameters for machining SHTSS using a rectangular graphite electrode were determined to be the highest settings for pulse current, spark-on time, and gap voltage.

These findings provide a practical framework for improving the productivity and efficiency of sinker-EDM applications, particularly for industries that require high-precision machining of challenging materials.

Author's Declaration

Authors' contributions and responsibilities

The authors played a significant role in the conception and design of this study. The authors also took responsibility for the data analysis, interpretation, and discussion of the results. All authors have reviewed and approved the final manuscript.

Acknowledgment

This research was fully funded by the Ministry of Education and Culture through the Novice Lecturer Research Program under contract number 106/E5/PG.02.00.PL/2024 (June 11, 2024) and 106/SP2H/RT-MONO/LL4/2024 (June 14, 2024). Special thanks to all the parties who contributed to this research, enabling the collection of comprehensive data.

Availability of data and materials

All data are available from the corresponding authors.

Competing interests

The authors declare that they have no conflicts of interest.

REFERENCES

- [1] E. C. Jameson, C. Zupan, Ed. *Electrical Discharge Machining*. Michigan: Machining Technology Association/SME, 2001
- [2] N. K. Singh and Y. Singh, "Experimental Investigation and Modeling of Surface Finish in Argon-Assisted Electrical Discharge Machining Using Dimensional Analysis," *Arabian Journal for Science and Engineering*, vol. 44, no. 6, pp. 5839-5850, (2019). doi: 10.1007/s13369-019-03738-5
- [3] B. Fleming, *The Edm How-To Book*. Fleming Publications, 2005
- [4] G. Kibria and B. Bhattacharyya, "Microelectrical discharge machining of Ti-6Al-4V," in *Microfabrication and Precision Engineering*, 2017, pp. 99-142. doi: 10.1016/b978-0-85709-485-8.00004-8
- [5] J. Vora, S. Khanna, R. Chaudhari, V. K. Patel, S. Paneliya, D. Y. Pimenov, K. Giasin, and C. Prakash, "Machining parameter optimization and experimental investigations of nano-graphene mixed electrical discharge machining of nitinol shape memory alloy," *Journal of Materials Research and Technology*, vol. 19, pp. 653-668, (2022). doi: 10.1016/j.jmrt.2022.05.076
- [6] R. Sheshadri, M. Nagaraj, A. Lakshmikanthan, M. P. G. Chandrashekarappa, D. Y. Pimenov, K. Giasin, R. V. S. Prasad, and S. Wojciechowski, "Experimental investigation of selective laser melting parameters for higher surface quality and microhardness properties: taguchi and super ranking concept approaches," *Journal of Materials Research and Technology*, vol. 14, pp. 2586-2600, (2021). doi: 10.1016/j.jmrt.2021.07.144
- [7] E.-H. Hasan, *Fundamentals of Machining Processes Conventional and Nonconventional Processes*, Third ed. Boca Raton: CRC Press, 2019
- [8] C. C. Wang and B. H. Yan, "Blind-hole drilling of Al₂O₃/6061Al composite using rotary electro-discharge machining," *Journal of Materials Processing Technology*, vol. 102, pp. 90-102, (2000). doi: [https://doi.org/10.1016/S0924-0136\(99\)00423-9](https://doi.org/10.1016/S0924-0136(99)00423-9)
- [9] N. M. Elsit, M. Y. Noordin, and A. U. Alkali, "Fabrication of high aspect ratio micro electrode by using EDM," in *IOP Conference Series: Materials Science and Engineering*, 2016, vol. 114. doi: 10.1088/1757-899x/114/1/012046
- [10] K. Khoirudin, S. Sukarman, N. Rahdiana, A. Suhara, and A. Fauzi, "Optimization of S-EDM Process Parameters on Material Removal Rate Using Copper Electrodes," *Jurnal Polimesin*, vol. 21, no. 1, (2023). doi: <http://dx.doi.org/10.30811/jpl.v21i1.3199>
- [11] M. Habib, "Microelectrochemical Deposition," in *Comprehensive Materials Processing*, vol. 11: Elsevier, 2014, pp. 11-523-V11-545. doi: <https://doi.org/10.1016/B978-0-08-096532-1.01109-2>

- [12] G. R. Ribeiro, I. M. F. Bragança, P. A. R. Rosa, and P. A. F. Martins, "A laboratory machine for micro electrochemical machining," in *Machining and machine-tools*: Woodhead Publishing Limited, 2013, pp. 195-210. doi: <https://doi.org/10.1533/9780857092199.195>
- [13] P. Sahoo and T. K. Barman, "ANN modelling of fractal dimension in machining," in *Mechatronics and Manufacturing Engineering*, J. P. Davim, Ed. Oxford: Woodhead Publishing, 2012, pp. 159-226. doi: <https://doi.org/10.1533/9780857095893.159>
- [14] R. Świercz, D. Oniszczyk-Świercz, L. Dąbrowski, and J. Zawora, "Optimization of machining parameters of electrical discharge machining tool steel 1.2713," 2018. doi: 10.1063/1.5056295
- [15] E. Aliakbari and H. Baseri, "Optimization of machining parameters in rotary EDM process by using the Taguchi method," *The International Journal of Advanced Manufacturing Technology*, vol. 62, no. 9-12, pp. 1041-1053, (2012). doi: 10.1007/s00170-011-3862-9
- [16] T. Sultan, A. Kumar, and R. D. Gupta, "Material Removal Rate, Electrode Wear Rate, and Surface Roughness Evaluation in Die Sinking EDM with Hollow Tool through Response Surface Methodology," *International Journal of Manufacturing Engineering*, vol. 2014, pp. 1-16, (2014). doi: 10.1155/2014/259129
- [17] S. Chandramouli and K. Eswaraiah, "Optimization of EDM Process parameters in Machining of 17-4 PH Steel using Taguchi Method," *Materials Today: Proceedings*, vol. 4, no. 2, pp. 2040-2047, (2017). doi: 10.1016/j.matpr.2017.02.049
- [18] S. Sumanto, A. Maulana, D. Mulyadi, K. Khoirudin, S. Siswanto, S. Sukarman, A. Suhara, and S. Safril, "Enhancement Material Removal Rate Optimization of Sinker-EDM Process Parameters Using a Rectangular Graphite Electrode," *Jurnal Optimasi Sistem Industri*, vol. 21, no. 2, pp. 87-96, (2022). doi: 10.25077/josi.v21.n2.p87-96.2022
- [19] I. A. Daniyan, K. Mpofu, and A. O. Adeodu, "Optimization of welding parameters using Taguchi and response surface methodology for rail car bracket assembly," *The International Journal of Advanced Manufacturing Technology*, vol. 100, no. 9-12, pp. 2221-2228, (2018). doi: 10.1007/s00170-018-2878-9
- [20] N. Yuvaraj, R. Arshath Raja, P. Palanivel, and N. V. Kousik, "EDM Process by Using Copper Electrode with INCONEL 625 Material," *IOP Conference Series: Materials Science and Engineering*, vol. 811, no. 1, (2020). doi: 10.1088/1757-899x/811/1/012011
- [21] S. Prasad Arikatla, K. Tamil Mannan, and A. Krishnaiah, "Parametric Optimization in Wire Electrical Discharge Machining of Titanium Alloy Using Response Surface Methodology," *Materials Today: Proceedings*, vol. 4, no. 2, pp. 1434-1441, (2017). doi: 10.1016/j.matpr.2017.01.165
- [22] *JIS G 4404: Alloy tool steels*, 2015.
- [23] S. Sukarman, A. Abdulah, A. D. Shieddieque, N. Rahdiana, and K. Khoirudin, "OPTIMIZATION OF THE RESISTANCE SPOT WELDING PROCESS OF SECC-AF AND SGCC GALVANIZED STEEL SHEET USING THE TAGUCHI METHOD," *SINERGI*, vol. 25, no. 3, pp. 319-328, (2021). doi: <http://10.22441/sinergi.2021.3.009>
- [24] F. Mucharom, R. L. Azizah, A. Suhara, N. Fazrin, A. Amir, B. Kristiawan, T. Triyono, and S. Sukarman, "Tensile shear load in resistance spot welding of dissimilar metals: An optimization study using response surface methodology," *Mechanical Engineering for Society and Industry*, vol. 3, no. 2, pp. 66-77, (2023). doi: 10.31603/mesi.9606
- [25] S. Sukarman, A. Shieddieque, C. Anwar, N. Rahdiana, and A. Ramadhan, "Optimization of powder coating process parameters in mild steel (SPCC-SD) to improve dry film thickness," *Journal of Applied Engineering Science*, vol. 19, no. 2, pp. 475-482, (2021). doi: 10.5937/jaes0-26093
- [26] P. Shandilya, P. K. Jain, and N. K. Jain, "Parametric Optimization During Wire Electrical Discharge Machining using Response Surface Methodology," *Procedia Engineering*, vol. 38, pp. 2371-2377, (2012). doi: 10.1016/j.proeng.2012.06.283

- [27] Minitab. (2023, 10/12/2023). *Overview for Probability Plot*.
- [28] A. G. Thakur and V. M. Nandedkar, "Optimization of the Resistance Spot Welding Process of Galvanized Steel Sheet Using the Taguchi Method," *Arabian Journal for Science and Engineering*, vol. 39, no. 2, pp. 1171-1176, (2013). doi: 10.1007/s13369-013-0634-x
- [29] K. Vignesh, A. Elaya Perumal, and P. Velmurugan, "Optimization of resistance spot welding process parameters and microstructural examination for dissimilar welding of AISI 316L austenitic stainless steel and 2205 duplex stainless steel," *The International Journal of Advanced Manufacturing Technology*, vol. 93, no. 1-4, pp. 455-465, (2017). doi: 10.1007/s00170-017-0089-4
- [30] P. Muthu, "Optimization of the Process Parameters of Resistance Spot Welding of AISI 316L Sheets Using Taguchi Method," *Mechanics and Mechanical Engineering*, vol. 23, no. 1, pp. 64-69, (2019). doi: 10.2478/mme-2019-0009
- [31] A. Moghanizadeh, "Reducing side overcut in EDM process by changing electrical field between tool and work piece," *The International Journal of Advanced Manufacturing Technology*, vol. 90, no. 1-4, pp. 1035-1042, (2016). doi: 10.1007/s00170-016-9427-1
- [32] M. F. Adnan, A. B. Abdullah, and Z. Samad, "Springback behavior of AA6061 with non-uniform thickness section using Taguchi Method," *The International Journal of Advanced Manufacturing Technology*, vol. 89, no. 5-8, pp. 2041-2052, (2016). doi: 10.1007/s00170-016-9221-0
- [33] A. A. A. Alduroobi, A. M. Ubaid, M. A. Tawfiq, and R. R. Elias, "Wire EDM process optimization for machining AISI 1045 steel by use of Taguchi method, artificial neural network and analysis of variances," *International Journal of System Assurance Engineering and Management*, vol. 11, no. 6, pp. 1314-1338, (2020). doi: 10.1007/s13198-020-00990-z
- [34] G. Smith, "Multiple Regression," in *Essential Statistics, Regression, and Econometrics*, 2012, pp. 297-331. doi: 10.1016/b978-0-12-382221-5.00010-6
- [35] D. L. Mohr, W. J. Wilson, and R. J. Freund, "Multiple Regression," in *Statistical Methods*, 2022, pp. 351-444. doi: 10.1016/b978-0-12-823043-5.00008-4
- [36] T. Y. Badgujar and V. P. Wani, "Stamping Process Parameter Optimization with Multiple Regression Analysis Approach," *Materials Today: Proceedings*, vol. 5, no. 2, pp. 4498-4507, (2018). doi: 10.1016/j.matpr.2017.12.019
- [37] H. Saini, I. Khan, S. Kumar, and S. Kumar, "Optimization of Material Removal Rate of WEDM Process on Mild Steel Using Molybdenum Wire," *International Journal of Advanced Engineering, Management and Science*, vol. 3, no. 10, pp. 1001-1005, (2017). doi: 10.24001/ijaems.3.10.5
- [38] A. Kumar, T. Soota, and J. Kumar, "Optimisation of wire-cut EDM process parameter by Grey-based response surface methodology," *Journal of Industrial Engineering International*, vol. 14, no. 4, pp. 821-829, (2018). doi: 10.1007/s40092-018-0264-8
- [39] S. Gopalakannan and T. Senthilvelan, "Optimization of machining parameters for EDM operations based on central composite design and desirability approach," *Journal of Mechanical Science and Technology*, vol. 28, no. 3, pp. 1045-1053, (2014). doi: 10.1007/s12206-013-1180-x
- [40] R. Bobbili, V. Madhu, and A. K. Gogia, "Modelling and analysis of material removal rate and surface roughness in wire-cut EDM of armour materials," *Engineering Science and Technology, an International Journal*, vol. 18, no. 4, pp. 664-668, (2015). doi: 10.1016/j.jestch.2015.03.014